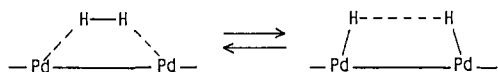


From these results, we conclude that the interaction of the hydrogen molecule with palladium is attractive and that the Pd<sub>2</sub> system is the smallest possible system that shows the catalytic activity for the dissociative adsorption of the H<sub>2</sub> molecule. The H<sub>2</sub> molecule with a binding energy of about 104 kcal/mol is dissociated, with almost no barrier, into two atomic hydrogens on the Pd<sub>2</sub> "surface", like on an extended surface.

From Figure 2, we see that the excited states of the Pd<sub>2</sub>-H<sub>2</sub> system are well separated from the ground state, throughout the process, by more than 50 kcal/mol. There is almost no chance for the excited states to participate in the dissociative process. Therefore, we conclude that the mechanism of the dissociative adsorption of the H<sub>2</sub> molecule on the Pd surface is different from that proposed for a Ni surface by Melius et al.<sup>4</sup>

Then, by what mechanism does the Pd<sub>2</sub> show such a catalytic ability? In Figure 3, we have shown a schematic orbital correlation diagram of the Pd<sub>2</sub>-H<sub>2</sub> system. It is based on the analysis of the natural orbitals of the MC-SCF calculations. The left-hand side is the MO's of H<sub>2</sub>, the right-hand side is the valence MO's of Pd<sub>2</sub>, and the center is for the Pd<sub>2</sub>H<sub>2</sub> system. Two interactions are important. One is the electron transfer from the δ<sub>u</sub>(d-d\*) MO of Pd<sub>2</sub> to the antibonding MO of H<sub>2</sub>. This transfer works to weaken the H-H bond. The other is the electron back-transfer from the bonding MO of H<sub>2</sub> to the bonding σ<sub>g</sub>(5s-5s) MO of Pd<sub>2</sub>. This back-transfer also works to weaken the H-H bond. These interactions increase as the H<sub>2</sub> approaches the Pd<sub>2</sub>, and finally lead to a cleavage of the H-H bond. Other implications of this diagram are that the d electrons are important in the newly formed Pd-H bond and that the Pd-Pd bond is *not* weakened (rather strengthened) by the adsorption of H<sub>2</sub>. The last point is because, on the Pd<sub>2</sub> side, the electron goes out from the antibonding δ<sub>u</sub> MO and comes in to the bonding σ<sub>g</sub> MO. This aspect seems to be important in relation to the stability of the catalyst, implying that the Pd atom is not exfoliated as a PdH molecule from the metal surface. We note that these 4d<sub>δ</sub> and 5s AO's constitute the so-called "dangling" bonds of the metal surface. This mechanism may be simplified as the bond alternation mechanism shown below.



We have obtained a density profile which confirms such a bond alternation.

The present result that even Pd<sub>2</sub> has catalytic activity for the H<sub>2</sub> cleavage shall suggest a design of the palladium catalyst not as a solid but in a more "molecular" form. Molecular beam experiment will also be interesting.

Lastly, we briefly summarize the calculational method used. The accuracy of the method was tested for the PdH molecule.<sup>13-15</sup> The Gaussian basis set for the Pd atom is a (3s3p3d)/[3s2p2d] set and the Kr core was replaced by an effective core potential.<sup>16</sup> For hydrogen, we used the (4s)/[2s] set of Huzinaga-Dunning<sup>17</sup> plus p-type functions which are the first derivatives of the [2s] set. The Hellmann-Feynman theorem is then essentially satisfied for the force acting on the hydrogen nuclei.<sup>18</sup> In the CAS-MC-SCF calculation,<sup>6</sup> we used a modified version of the GAMESS

program<sup>19</sup> and adopted 8 (lower) × 2 (upper) active orbital spaces for Pd<sub>2</sub>H<sub>2</sub>. The SAC and SAC-CI methods<sup>10,11</sup> include a much larger amount of electron correlation than the MC-SCF method. More details will be given elsewhere in the literature.

**Acknowledgment.** We acknowledge Professor T. Yonezawa for interest and encouragement. The calculations were carried out at the Data Processing Center of Kyoto University and at the Computer Center of the Institute for Molecular Science. Part of this study was supported by the Grant-in-Aid for the Scientific Research from the Ministry of Education, Science, and Culture.

(19) Brooks, B. R.; Saxe, P.; Laidig, W. D.; Dupuis, M. Program System GAMESS, Program Library No. 481, Computer Center of the Institute for Molecular Science, 1981.

## Sequence-Specific Cleavage of Double-Helical DNA. N-Bromoacetyldistamycin

Brenda F. Baker and Peter B. Dervan\*

Division of Chemistry and Chemical Engineering  
California Institute of Technology  
Pasadena, California 91125

Received July 19, 1985

The modification of double-helical DNA by electrophiles which results in cleavage of the DNA backbone has played a useful role in the chemical sequencing of nucleic acids.<sup>1</sup> Certain natural products such as CC-1065,<sup>2</sup> mitomycin,<sup>3</sup> and anthramycins<sup>4</sup> react with specific sequences of double-helical DNA by electrophilic attack. One approach for the design of synthetic sequence-specific DNA cleaving molecules would be attachment of electrophiles to sequence-specific DNA binding molecules. Proper positioning of the electrophile near nucleophilic centers on DNA such as N3 of adenine in the minor groove of DNA or N7 of guanine in the major groove of DNA would require some understanding of the molecular structure of the DNA binding unit complexed to the DNA double helix.<sup>5</sup> We have shown previously, by footprinting<sup>6,7</sup>

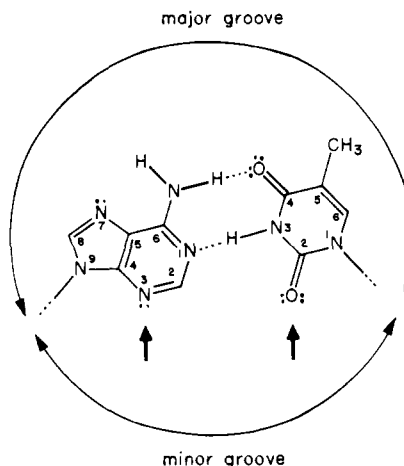
(1) (a) For example, dimethyl sulfate alkylates N7 of guanine in the major groove of DNA. Maxam, A. M.; Gilbert, W. *Methods Enzymol.* **1980**, *65*, 499-560. (b) Lawley, P. D.; Brookes, P. *Biochem. J.* **1963**, *89*, 127-138.

(2) Hurley, L. H.; Reynolds, V. L.; Swenson, D. H.; Petzold, G. L.; Scallion, T. A. *Science (Washington, D.C.)* **1984**, *226*, 843-844 and references cited therein.

(3) Ueda, K.; Morita, J.; Komano, T. *Biochemistry* **1984**, *23*, 1634-1640 and references cited there. (b) Komano, T.; Ueda, K.; *Nucl. Acids Res.* **1984**, *12*, 6673-6683. (c) Tomasz, M.; Lyman, R.; Snyder, J. K.; Nakanishi, K. *J. Am. Chem. Soc.* **1983**, *105*, 2059-2063.

(4) (a) Petrussek, R. L.; Anderson, G. L.; Garner, T. F.; Fannin, Q. L.; Kaplan, D. J.; Zimmer, S. G.; Hurley, L. H. *Biochemistry* **1981**, *20*, 1111-1119. (b) Graves, D. E.; Pattaroni, C.; Krishnan, B. S.; Ostrand, J. M.; Hurley, L. H.; Krugh, T. R. *J. Biol. Chem.* **1984**, *259*, 8202-8209.

(5) Arrows indicate potential sites for electrophilic attack at N3 of adenine and O2 of thymine in the minor groove of the B DNA helix.



(13) To confirm the accuracy of the present calculational method, we carried out the CAS-MC-SCF calculation of the PdH molecule. The ground state was  $^2\Sigma^+$  in agreement with experiment. The calculated values of the equilibrium geometry, vibrational frequency, dissociation energy, and dipole moment are 1.570 Å (1.529 Å), 1496 cm<sup>-1</sup> (1446 cm<sup>-1</sup>), 54 kcal/mol (~76 kcal/mol), and 2.81 D (1.977 D), respectively, with the values in the parentheses being the experimental values.<sup>12,14</sup> The present result may also be compared with the result of Pacchioni, Koutecky, et al.<sup>3,15</sup>

(14) Malmberg, C.; Scullman, R.; Nylén, P. *Ark. Fys.* **1969**, *39*, 495.

(15) Pacchioni, G.; Koutecky, J.; Fantucci, P. *Chem. Phys. Lett.* **1982**, *92*, 486.

(16) Hay, P. J. *J. Am. Chem. Soc.* **1981**, *103*, 1390.

(17) (a) Huzinaga, S. *J. Chem. Phys.* **1965**, *42*, 1293. (b) Dunning, T. H., Jr. *J. Chem. Phys.* **1970**, *53*, 2823.

(18) (a) Nakatsuji, H.; Kanda, K.; Yonezawa, T. *Chem. Phys. Lett.* **1980**, *75*, 340. (b) Nakatsuji, H.; Hayakawa, T.; Hada, M. *Chem. Phys. Lett.* **1981**, *80*, 94. (c) Nakatsuji, H.; Kanda, K.; Hada, M.; Yonezawa, T. *J. Chem. Phys.* **1982**, *77*, 3109.

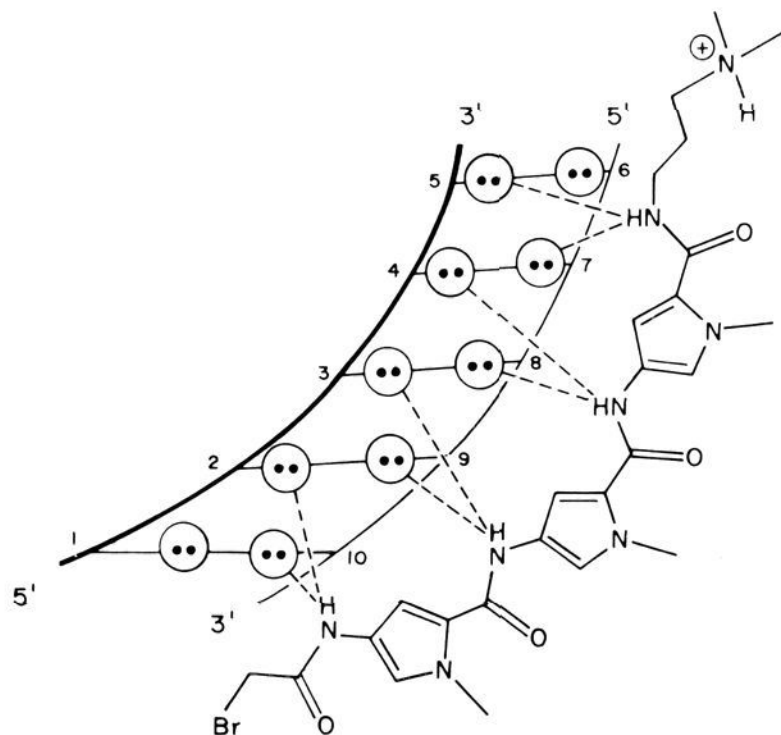


**Figure 1.** Model of the *N*-bromoacetyldistamycin (BD) bound to five base pairs of A + T in the minor groove of right-handed B DNA. Circles with two dots represent lone pairs of electrons on N3 of adenine and O2 of thymine at the edges of the base pairs on the floor of the minor groove of the DNA helix. Dotted lines are bridged hydrogen bonds to the amide NHs.

and affinity cleaving methods,<sup>7,8</sup> that the tripeptide unit from the natural product distamycin binds to five-base-pair sites with a preference for A·T rich regions. In most cases the tripeptide can adopt two orientations at each A·T rich binding site.<sup>7,8</sup> From the recent X-ray analysis of the complex of netropsin with the B DNA dodecamer of sequence CGCGAATTCGCG, Dickerson and co-workers provide a molecular basis for the sequence-specific recognition of DNA by netropsin and, by extension, distamycin.<sup>9</sup> They find that the crescent-shaped dipeptide sits symmetrically in the center of the minor groove of right-handed DNA and displaces the water molecules of the spine of the hydration.<sup>9</sup> Each of its three amide NH groups forms a bridge between adjacent adenine N3 or thymine O2 atoms on opposite helix strands.<sup>9</sup> From model-building studies, an electrophile attached to the terminal amide NH of tris-*N*-methylpyrrolicarboxamide would be proximal to the edges of the bases of the five-base-pair A·T rich binding site (Figure 1). If electrophilic attack occurs at adenine in the minor groove of B DNA<sup>5</sup> then under appropriate workup procedures, in depurination and DNA backbone cleavage might result at that site.<sup>10</sup>

We report that *N*-bromoacetyldistamycin (BD) which contains the electrophile bromoacetyl on the amino end of the tripeptide tris-*N*-methylpyrrolicarboxamide<sup>11</sup> cleaves a single adenine within a restriction fragment containing 167 base pairs of DNA after 5 h of reaction time at 37 °C followed by a depurination workup procedure.

(6) (a) Van Dyke, M. W.; Hertzberg, R. P.; Dervan, P. B. *Proc. Natl. Acad. Sci. U.S.A.* **1982**, *79*, 5470–5474. (b) Van Dyke, M. W.; Dervan, P. B. *Cold Spring Harbor Symp. Quant. Biol.* **1983**, *47*, 347–353. (c) Van Dyke, M. W.; Dervan, P. B. *Biochemistry* **1983**, *22*, 2373–2377. (d) Van Dyke, M. W.; Dervan, P. B. *Nucl. Acid Res.* **1983**, *11*, 5555–5567.

(7) Schultz, P. G.; Dervan, P. B. *J. Biomol. Struct. Dyn.* **1984**, *1*, 1133–1147.

(8) (a) Taylor, J. S.; Schultz, P. G.; Dervan, P. B. *Tetrahedron* **1984**, *40*, 457–465. (b) Youngquist, R. S.; Dervan, P. B. *Proc. Natl. Acad. Sci., U.S.A.* **1985**, *82*, 2565–2569.

(9) Kopka, M. L.; Yoon, C.; Goodsell, D. Pjura, P.; Dickerson, R. E. *Proc. Natl. Acad. Sci. U.S.A.* **1985**, *82*, 1376–1380.

(10) There are other nucleophilic sites in the minor groove of DNA such as O2 of thymine. N3 may not be the exclusive site of electrophilic attack, only one potential site for base labilization and DNA backbone cleavage.

(11) The NMR, IR, UV, and mass spectral data are consistent with the assigned structure. The synthetic details which are similar to methods described in ref 8a will be published in a full manuscript.

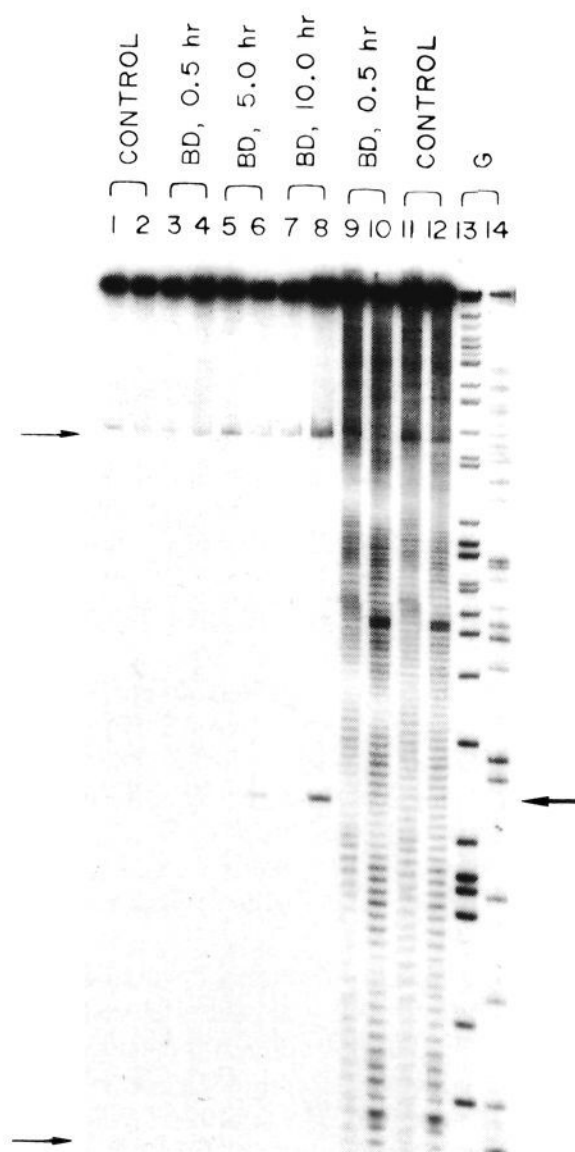


**Figure 2.** Autoradiogram of high-resolution denaturing gel. Odd- and even-numbered lanes are DNA end-labeled with <sup>32</sup>P at the 5' and 3' position, respectively. Arrows on the left of the autoradiogram reading bottom to top is the sequence left to right in Fig. 3. Arrow on the right at the middle of the gel is the site of major cleavage (see lane 8).

The tripeptide tris-*N*-methylpyrrolicarboxamide has been shown by footprinting and affinity cleaving methods to bind four five-base-pair sites on a 167-base DNA restriction fragment (Eco RI/Rsa I) from pBR322 plasmid DNA.<sup>7,8</sup> To test for sequence-specific cleavage of DNA, BD at 5.0 μM concentration was allowed to equilibrate at 37 °C (pH 7.0) with this <sup>32</sup>P end-labeled DNA restriction fragment (100 μM in base pairs of DNA).<sup>12</sup> After reaction times of 0.5, 5, and 10 h at 37 °C, the DNA was precipitated with EtOH. Following a modified Maxam–Gilbert DNA cleavage workup procedure, the DNA in each case was heated at 90 °C (15 min, phosphate buffer, pH 7.0) and then at 90 °C with piperidine (15 min).<sup>1</sup> At the 0.5-h reaction time (37 °C) after workup, no significant DNA cleavage was visualized on autoradiogram of the high-resolution denaturing electrophoresis gel (Figure 3, lanes 3, 4).<sup>13</sup> However, after 5- and 10-h reaction times (37 °C) followed by workup, analysis of the DNA cleavage products by high-resolution denaturing gel electrophoresis reveals major cleavage at a single adenine<sup>14</sup> (Figure 2, lanes 5–8). Footprinting with the synthetic DNA-cleaving reagent MPE-Fe<sup>II</sup>,<sup>6</sup> under conditions of little observable cleavage by BD (0.5 h, 37 °C) reveals that BD is binding four five-base-pair

(12) The reactions were run with >600 cpm of <sup>32</sup>P end-labeled restriction fragments made up to a total DNA concentration of 100 μM in base pairs with sonicated calf thymus DNA in 10 mM phosphate buffer (pH 7.0).

(13) After workup each reaction mixture was lyophilized and suspended in 4 μL of pH 8.3, 100 mM Tris-borate, 75% formamide solution. These solutions were heat denatured and loaded on a 0.4 mm thick, 40 cm long, 8% polyacrylamide, 1:20 cross-linked, and 50% urea gel and electrophoresed at 1200 V. Autoradiography of the gels was carried out at –50 °C on Kodak, X-Omat AR film, and the autoradiograms were scanned at 485 nm. The relative peak area for each site was equated to the relative cleavage efficiency.

(14) The location of this adenine on the plasmid pBR322 and the 167-bp restriction fragment is base-pair number 48.<sup>15</sup>

(15) Sutcliffe, J. G. *Cold Spring Harbor Symp. Quant. Biol.* **1979**, *43*, 77–90.

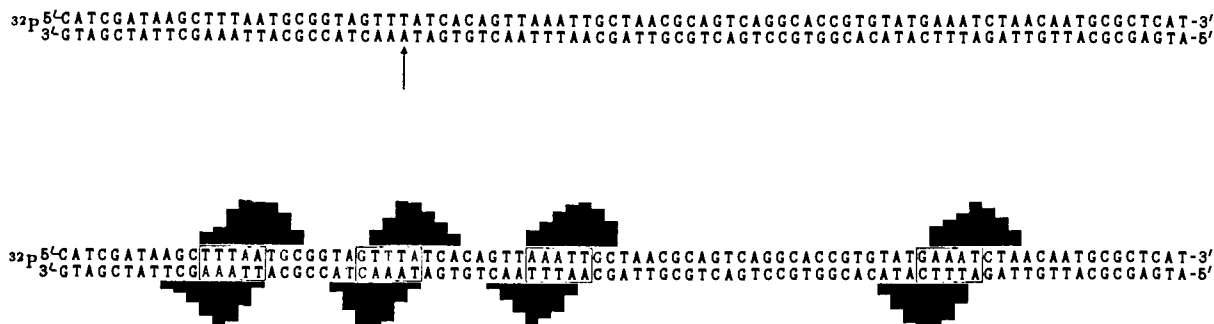


**Figure 3.** Base pairs 22–108 from pBR322 plasmid.<sup>15</sup> (Top) Arrow indicates major site of DNA cleavage<sup>14</sup> resulting from reaction with BD on 167-bp restriction fragment after 5 and 10 h at 37 °C (pH 7.0). (Bottom) MPE-Fe<sup>II</sup> footprints of BD at 5  $\mu$ M concentration bound to 167 bp restriction fragment at 37 °C (pH 7.0). Asymmetric histograms on each strand represent regions on the 5' (and 3') <sup>32</sup>P end-labeled DNA restriction fragment protected by BD from cleavage by MPE-Fe<sup>II</sup> (Fig. 2, lanes 9, 10). Boxes are equilibrium binding sites of BD whose assignment is based on the MPE-Fe<sup>II</sup> footprinting model described in ref 6b,c and 7.

sites at 5  $\mu$ M concentration on the 167 bp fragment (5'-3') TTTAA, GTTAA, AAATT, and GAAAT (Figure 3). These are the same sites bound by distamycin.<sup>7,8</sup> The major cleavage site is contained within one of these four equilibrium binding sites on the complementary strand of the 5'-GTTTA-3' site as shown by the arrow in Figure 3.<sup>14</sup> At reaction times longer than 10 h a second cleavage site becomes visible at the first adenine in the binding site, 5'-AAATT-3'.

An understanding of the mechanistic details by which the synthetic BD exhibits preferential cleavage at one of 334 nucleotides in the 167-bp DNA fragment<sup>14</sup> must await characterization of the DNA cleavage products<sup>16</sup> and kinetic analyses. From the MPE-Fe<sup>II</sup> footprinting results at 37 °C (0.5 h), we find that the *N*-bromoacetyl moiety has not changed significantly the equilibrium binding specificity of the tripeptide unit on DNA because we observe the same DNA binding sites for BD as the natural product distamycin. The few cleavage sites observed at 37 °C (5–10 h) may indicate unequal relative rates of reaction of a minimum of seven adenines proximal to the bound bromoacetyltripeptide within the four tripeptide equilibrium binding sites. If this is true, the different rates of reaction at proximal adenines may be a reflection of the sequence-dependent differences of local structure of B-form DNA<sup>9</sup> and the stereoelectronic requirement in the transition state for the backside nucleophilic displacement reaction. In fact, the synthetic bromoacetyldistamycin may mimic in mechanistic aspects the natural product antitumor agent CC-1065 which alkylates DNA at A·T rich regions five base pairs in size.<sup>2</sup>

Finally, we had previously reported that tris(*N*-methylpyrrolicarboxamide) equipped with EDTA·Fe<sup>II</sup>[distamycin-EDTA·Fe<sup>II</sup>] affords multiple cleavage patterns flanking both sides of a five-base-pair A·T rich binding site.<sup>8</sup> Because the bromoacetyl moiety is nondiffusible, the electrophilic-mediated cleavage affords single cleavage events within each equilibrium binding site which can be distinguished from the multiple cleavage loci caused by a diffusible oxidant generated by EDTA·Fe<sup>II</sup>. By changing the DNA cleaving function attached to the same DNA binding unit [tris(*N*-methylpyrrolicarboxamide)], from a *non-sequence-specific diffusible* oxidant to a *sequence-specific nondiffusible* electrophile, we find quite different levels of sequence-specific DNA cleavage. From the point of view of determining the sequence specificity of DNA binding molecules, the nonspecific DNA cleaving function EDTA·Fe<sup>II</sup> is preferred.<sup>17</sup> From the point of view of designing a very specific DNA cleaving molecule, the combination of a base-specific DNA cleaving moiety with a sequence-specific DNA binding unit affords a highly discriminating DNA cleaving

molecule.

**Acknowledgment.** We are grateful to the National Institutes of Health (GM-27681) for support of this research.

### NMR Evidence for a Horseradish Peroxidase State with a Deprotonated Proximal Histidine

Jeffrey S. de Ropp,<sup>1b</sup> V. Thanabal,<sup>1a</sup> and Gerd N. La Mar<sup>\*1a</sup>

Department of Chemistry and UCD NMR Facility  
University of California, Davis, California 95616

Received July 22, 1985

The modulation of heme iron reactivity in peroxidases by removal of the labile proton from the ubiquitous proximal histidine has long been postulated.<sup>2–5</sup> Both resonance Raman and electronic spectra of reduced horseradish peroxidase (HRP) have been interpreted in terms of a deprotonated proximal imidazole.<sup>6–9</sup> However, for both reduced- and resting-state HRP, the presence of this proton could be established in the <sup>1</sup>H NMR spectrum by its characteristic large downfield hyperfine shift,<sup>10–12</sup> as found in model compounds,<sup>13</sup> confirming the presence of an imidazole rather than an imidazolate as axial ligand in the five-coordinate state. Both functional states of HRP,<sup>2,5</sup> the enzymatic intermediates HRP compounds I and II, however, are six-coordinate, and little is known about the nature of the axial imidazole in such low-spin derivatives. While the relevant resonance Raman bands, to our knowledge, have not been located in any low-spin six-coordinate HRP complex, some indirect NMR data<sup>14</sup> on nonexchangeable protons have suggested extensive imidazolate character in the cyano complex HRPCN. Labile proton signals consistent with originating from the axial histidyl imidazole have been re-

- (1) (a) Department of Chemistry. (b) UCD NMR Facility.
- (2) Morrison, M.; Schonbaum, G. R. *Annu. Rev. Biochem.* **1976**, *45*, 861–888.
- (3) Nicholls, P. *Biochim. Biophys. Acta* **1962**, *60*, 217–228.
- (4) Blumberg, W. E.; Peisach, J. In "Probes of Structure and Function of Macromolecules and Membranes"; Chance, B., Yonetani, T., Mildvan, A. S., Eds.; Academic Press: New York, 1971; Vol. II, pp 215–229.
- (5) Schonbaum, G. R. In "Oxidases and Related Redox Systems"; King, E., Mason, H. S., Morrison, M., Eds.; Pergamon Press: Oxford, 1982; pp 671–684.
- (6) Stein, P.; Mitchell, M.; Spiro, T. G. *J. Am. Chem. Soc.* **1980**, *102*, 7795–7797.
- (7) Teraoka, J.; Kitagawa, T. *J. Biol. Chem.* **1981**, *256*, 3969–3977.
- (8) Desbois, A.; Mazza, G.; Stretzkowski, F.; Lutz, M. *Biochim. Biophys. Acta* **1984**, *785*, 161–176.
- (9) Mincey, T.; Traylor, T. G. *J. Am. Chem. Soc.* **1979**, *101*, 765–766.
- (10) La Mar, G. N.; de Ropp, J. S. *Biochem. Biophys. Res. Commun.* **1979**, *90*, 36–41.
- (11) La Mar, G. N.; de Ropp, J. S. *J. Am. Chem. Soc.* **1982**, *104*, 5203–5206.
- (12) La Mar, G. N.; de Ropp, J. S.; Smith, K. M.; Langry, K. C. *J. Biol. Chem.* **1980**, *255*, 6646–6652.
- (13) La Mar, G. N.; Budd, D. L.; Goff, H. *Biochem. Biophys. Res. Commun.* **1977**, *77*, 104–110.
- (14) La Mar, G. N.; de Ropp, J. S.; Chacko, V. P.; Satterlee, J. D.; Erman, J. E. *Biochim. Biophys. Acta* **1982**, *708*, 317–325.

(16) The DNA termini at the cleavage site are 5'-phosphate and 3'-phosphate. This is consistent with alkylation of adenine followed by depurination and deoxyribose hydrolysis to afford a "gap" at the cleavage site.

(17) The affinity cleaving technique simply takes advantage of the analytical power of high-resolution denaturing gel electrophoresis to determine the sequence specificities of equilibrium binding molecules on DNA.<sup>8</sup>